

A Study on the Iron Losses in Flux-Switching Permanent Magnet Machines

Heung-Kyo Shin[†]

Abstract – Flux-switching permanent magnet machines (FSPMM) have doubly-salient and simple structures making it cost effective and suitable for mass production. In addition, it is possible to increase the rotor rotating speed and concentrate the flux of the permanent magnet on the air-gap. Due to these merits, the FSPMM can be applied to the various industry applications. To improve the performance, various design variables need to be studied in terms of design techniques. In this paper, we especially concentrate on the distribution of iron losses using a two-dimensional finite-element method (2D FEM). As a result, we can get an information for high efficiency FSPMM design.

Keywords: Flux-switching permanent magnet machine (FSPMM), Two-dimensional finite element method (2D-FEM), Iron losses, Eddy current loss, Hysteresis loss

1. Introduction

THE MACHINES with permanent magnets on their internal rotor need to protect magnets from the centrifugal force for high-speed applications. Therefore, most of them have a retaining sleeve made of either stainless steel or non-metallic fiber. This sleeve make air-gap larger in magnetic circuit and deteriorate the performances of the machine such as efficiency and power density. The running temperature rise in the rotor may also be a problem because of poor thermal dissipation, which cause irreversible demagnetization of the permanent magnets and decrease the magnetic torque and power density of the machine. To overcome these disadvantages, some novel topologies of machines have been proposed [1-3]. Among them, flux-switching permanent magnet machines (FSPMM) have doubly-salient stator and rotor structures and employ concentrated windings and permanent magnets in the stator, which lead to low copper consumption and loss, low self and mutual inductances, low electrical time constant and high fault tolerance [4-7].

However, despite of their advantages, the design methods to get high efficiency have not been studied and reported. Generally, in most electrical machines, iron losses play a key role in getting high efficiency, which means that it is very important to get an information about the iron losses precisely.

In this paper, we analyze the precise distributions of the iron losses in the 3-phase, 12/10-pole FSPMM using a two-dimensional finite-element method (2D FEM). The iron losses are directly calculated and predicted from the instantaneous time variation of the magnetic field distribution. As a result, we present the design variables that have the

largest effect on the iron losses and an information for high efficiency design.

2. The Analysis Model

2.1 The Prototype FSPMM

Fig. 1 shows the cross-sections of a 3-phase, 12/10-pole FSPMM. The rotor is the same 'as that of a switched reluctance (SR) machine. The stator employs 12 segments of U-shape magnetic cores and 12 pieces of inset magnets. The magnets are magnetized circumferentially in alternative opposite directions. The permanent magnet material is sintered Nd-Fe-B and the thickness is 2 mm. The important

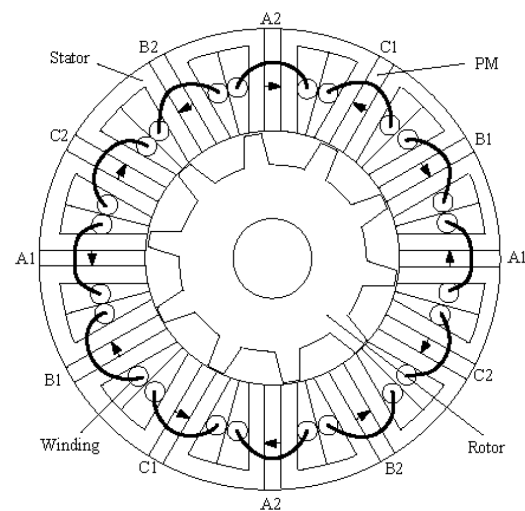


Fig. 1. The 3-phase, 12/10-pole FSPMM.

[†] Corresponding Author: Dept. of Electrical Engineering, Engineering Research Institute, Gyeongsang National University, Korea. (hkshin@gnu.ac.kr)

Received: September 6, 2017; Accepted: December 6, 2017

Table 1. Specifications of the prototype FSPMM

Section	Item	Value	(Unit)
Stator	Number of phases	3	
	Number of slots	12	
	Outer diameter	160	(mm)
	Stack width	47.5	(mm)
	Number of turns/phase/pole	50	(turns)
Rotor	Number of poles	10	
	Outer diameter	80	(mm)
	Inner diameter	30	(mm)
	Pole length	5.5	(mm)
Rated	Power	1200	(W)
	Speed	1000	(rpm)
	Current	10	(Arms)
Etc.	Mechanical air gap	0.5	(mm)
	Insulation grade	H	
	Steel	S23	



Fig. 2. Air-gap flux density waveforms.

FSPMM design specifications are given on Table 1.

2.2 The basic characteristics of the prototype FSPMM

Fig. 2 shows the air-gap flux density waveform at no load. We can see that the radial component is bigger than the tangential one. They also have a lot of space harmonics. Fig. 3 and Fig. 4 show the Back-EMF waveforms at 1000 rpm and cogging torque, respectively. If the FSPMM is driven by the sinewave currents, the harmonics of the Back-EMF should be diminished. The cogging torque that can generate vibrations and additional noises is also big. So, the effort to decrease the cogging torque is necessarily needed to improve performances.

3. 2-Dimensional Finite Element Method

3.1 Governing equation and discretization

The two-dimensional governing equation for the FRM can be expressed in magnetic vector potential A by the

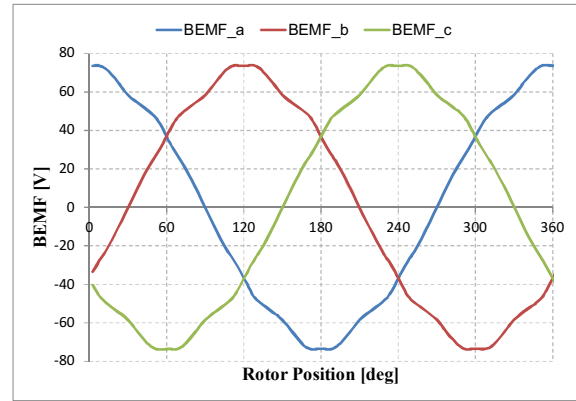


Fig. 3. BEMF waveforms at 1500 rpm.

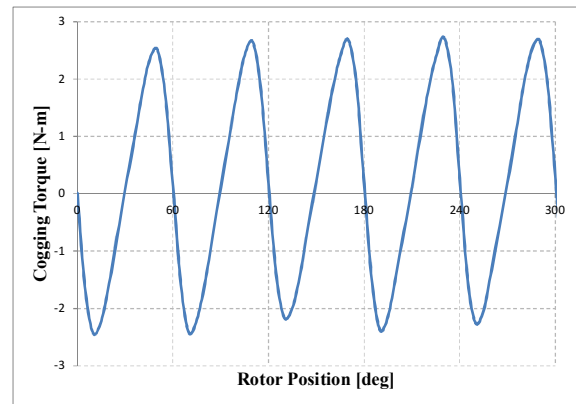


Fig. 4. Cogging torque waveform.

following.

$$\frac{\partial}{\partial x} \left(\frac{1}{\mu} \frac{\partial A_z}{\partial x} \right) + \frac{\partial}{\partial y} \left(\frac{1}{\mu} \frac{\partial A_z}{\partial y} \right) = -J_0 - \frac{1}{\mu_0} \left(\frac{\partial M_y}{\partial x} - \frac{\partial M_x}{\partial y} \right) \quad (1)$$

where A_z is the z -component of the magnetic vector potential, J_0 is current density, and M is the magnetization of a permanent magnet.

Applying the Galerkin's method to (1), we can obtain a finite element equation in a first order triangular element as follows:

$$I_{ie} = \int_{Se} \frac{1}{\mu} \left\{ \sum_{j=1}^3 \left(\frac{\partial N_{ie}}{\partial x} \frac{\partial N_{je}}{\partial x} + \frac{\partial N_{ie}}{\partial y} \frac{\partial N_{je}}{\partial y} \right) A_{je} \right\} dx dy - \int_{Se} \frac{1}{\mu_0} \left(M_x^e \frac{\partial N_{ie}}{\partial y} - M_y^e \frac{\partial N_{ie}}{\partial x} \right) dx dy - \int_{Se} J_0 N_{ie} dx dy \quad (2)$$

where N stands for a shape function.

3.2 The iron losses analysis

After getting the variance of the distribution of the magnetic flux density from the 2D FEM, we calculate the iron losses (the eddy current and hysteresis losses). The

eddy current loss can be expressed as Eq. (3).

$$w_{ie} = \frac{k_e d}{2\pi^2} \int_{iron} \frac{1}{N} \sum_{k=1}^N \left\{ \left(\frac{B_r^{k+1} - B_r^k}{\Delta t} \right)^2 + \left(\frac{B_\theta^{k+1} - B_\theta^k}{\Delta t} \right)^2 \right\} dv \quad (3)$$

where, k_e is the eddy current loss coefficient, Δt is the time interval of data, and N is the number of recurrence calculations.

If a magnetic field has time and space harmonics, the hysteresis loss become larger due to additional minor loops. Accordingly, in order to calculate an accurate hysteresis loss, both major and minor loops should be considered. We also assume that every maximum and minimum value of the flux density make hysteresis loops and the shape of each loop is the same as the fundamental hysteresis loop. The hysteresis loss can be expressed as Eq. (4) by using the hysteresis loss coefficient k_h [8, 9].

$$w_{ih} = \frac{k_h d}{T} \sum_{k=1}^{NE} \frac{\Delta V_i}{2} \left\{ \sum_{j=1}^{Np_r^i} (B_{mr}^{ij})^2 + \sum_{j=1}^{Np_\theta^i} (B_{m\theta}^{ij})^2 \right\} \quad (4)$$

Where NE is the number of finite element of the iron, ΔV_i is the volume that corresponds to the i -th finite element, Np_r^i , Np_θ^i are the appearing numbers of local maximum and local minimum of i -th finite element which has time varying flux of r , θ directions, and B_{mr}^{ij} , $B_{m\theta}^{ij}$ are the amplitudes of the hysteresis loop.

4. Analysis Results

Fig. 5 and 6 illustrate the flux density variation and contour in the stator yoke, respectively. The flux from stator teeth passes through the stator yoke. Therefore, the theta (tangential) component of the flux is a majority. From the contour of the flux density, we can see that the stator yoke has an alternating magnetic field. Generally, it says

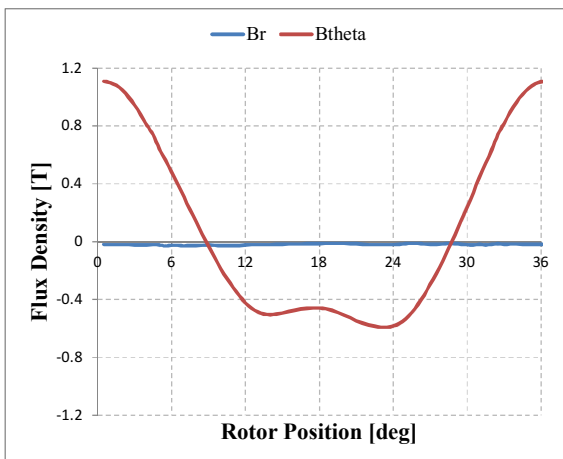


Fig. 5. Flux density variations in the stator yoke.

that this alternating field makes less iron losses than a rotating field. Fig. 7 and 8 show the case of the stator teeth. The radial component of the flux is bigger than the tangential component. The magnetic field is also alternating like the yoke. From the graphs, it is possible to know that the eddy current loss of the stator teeth can be larger than that of the yoke. This is due to the large variation of magnetic flux density in the teeth part.

Fig. 9, 10, 11, and 12 show the flux density variations and contours in the rotor yoke and teeth, respectively. The variations of the flux density are larger than that of the stator. Both the yoke and teeth in the rotor have a rotating magnetic field, which can produce much iron losses. There are also at least two minor hysteresis loops in the yoke and teeth part. These loops generate additional hysteresis losses. Accordingly, the hysteresis losses are larger than the eddy current losses in the case of the rotor.

Despite the rotor has the rapid variations and a rotating field, the total iron losses of the rotor can be smaller than that of the stator. This is because the amount of the used iron in the rotor is small.

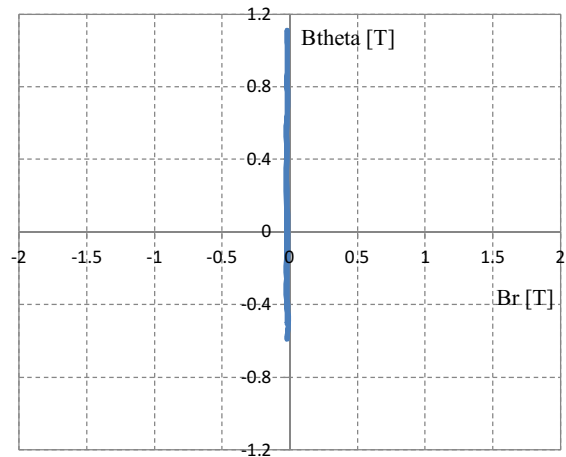


Fig. 6. Flux density contour in the stator yoke.

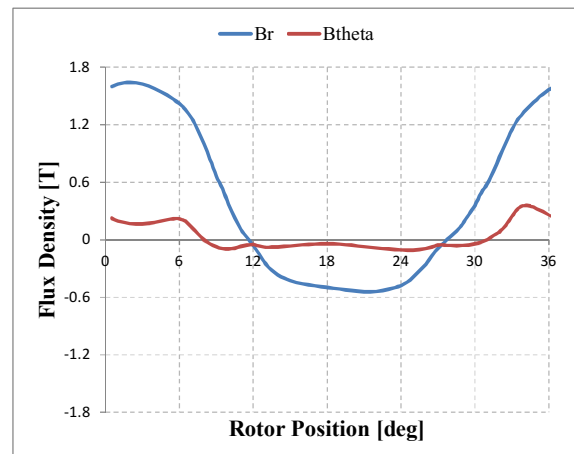


Fig. 7. Flux density variations in the stator teeth.

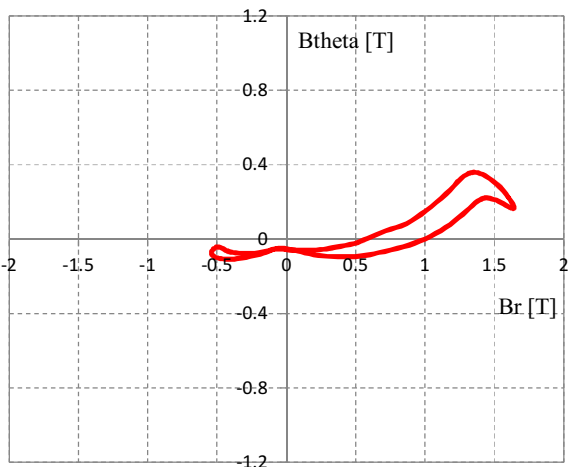


Fig. 8. Flux density contour in the stator teeth.

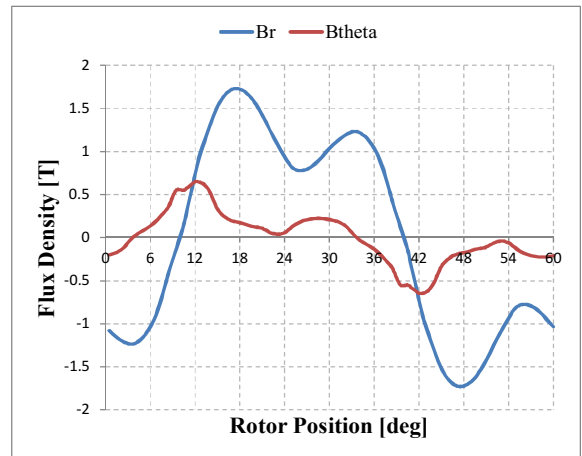


Fig. 11. Flux density variations in the rotor teeth.

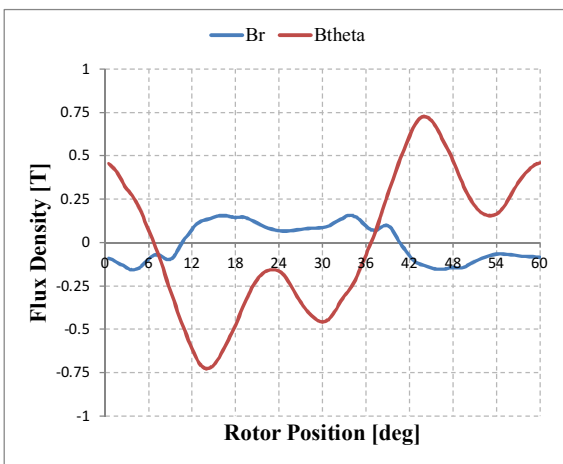


Fig. 9. Flux density variations in the rotor yoke.

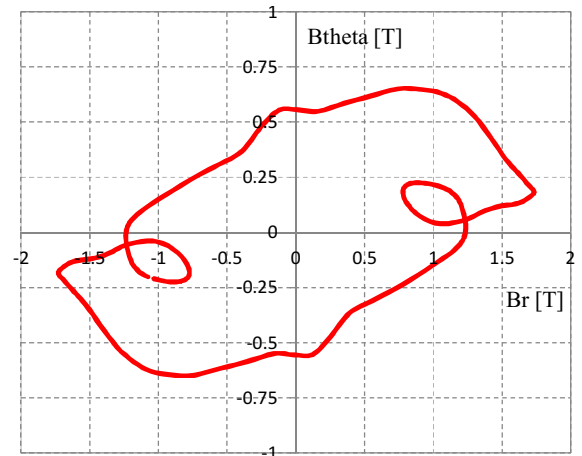


Fig. 12. Flux density contour in the rotor teeth.

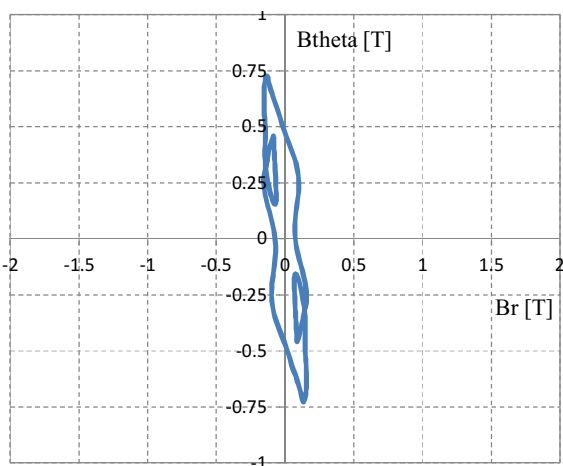


Fig. 10. Flux density contour in the rotor yoke.

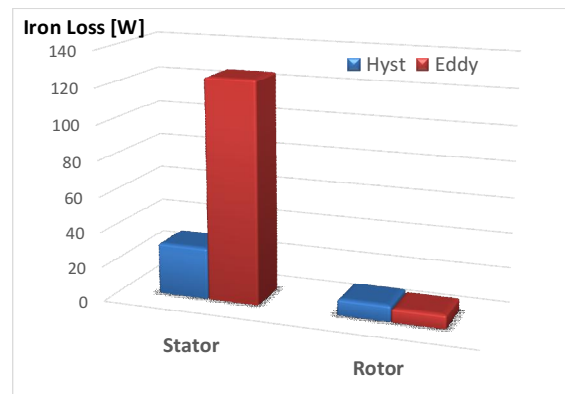


Fig. 13. The calculation results of iron losses.

Fig. 13 compares the calculated iron losses at the rated output and rotating speed. In the case of stator, the eddy current loss is much larger than the hysteresis loss, while the rotor has larger hysteresis loss. This is due to the fact

that the variation of flux density in the stator varies rapidly and the rotor has a rotating field. Fig. 14 shows the distribution of the iron loss density. From this figure, we can see that most iron losses concentrate on the stator teeth part and the top area of the rotor teeth. Accordingly, to decrease the iron losses and get higher efficiency, we need to optimize the shape of the teeth. It is especially important

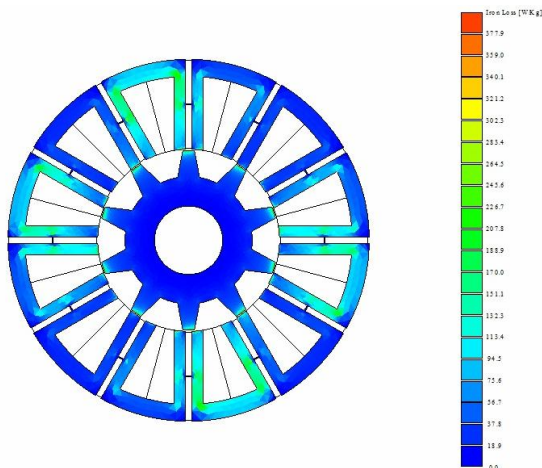


Fig. 14. The distribution of the iron loss density.

to diminish the harmonics of the flux density in the top part of the rotor teeth.

5. Conclusion

Decreasing the hysteresis and eddy current losses in the iron consists of a magnet circuit is very important in designing a flux-switch permanent magnet machine for high efficiency. In this paper, the analysis and distribution of the iron losses have been investigated. To get an accurate calculation, we have used 2-D finite element method. From the analysis results, we can know that the teeth shapes in the stator and rotor are the most important and effective design variables to decrease the iron losses. These results could be adopted to design the FSPMM with high efficiency and power density.

References

- [1] S. E. Rauch and L. J. Johnson, "Design principles of flux-switching alternators," *AIEE Trans. 74III*, pp. 1261-1268, 1995.
- [2] Y. Liao, F. Liang, and T. A. Lipo, "A novel permanent-magnet motor with doubly-salient structure," *IEEE Transactions on Industrial Applications*, vol. 31, no. 5, pp. 1069-1078, Sept./Oct. 1995.
- [3] M. Cheng, K. T. Chau, and C. C. Chan, "Static characteristics of a new doubly salient permanent magnet machine," *IEEE Transaction on Energy Conversion*, vol. 16, no. 1, pp. 20-25, 2001.
- [4] E. Hoang, A. H. Ben-Ahmed, and J. Lucidarme, "Switching flux permanent magnet polyphased machines," *EPE'97 7th European Conf. Power Electronic and Applications*, vol. 3, pp. 903-908, 1997.
- [5] E. Hoang, M. Gabsi, M. Lecrivain, and B. Multon, "Influence of magnetic losses on maximum power limits of synchronous permanent magnet drives in flux-weakening mode," *Proc. IEEE IAS 2000 Annual Conf.*, vol. 1, pp. 299-303, 2000.
- [6] Y. Amara, E. Hoang, M. Gabsi, M. Lecrivain, and S. Allano, "Design and comparison of different flux-switch synchronous machines for an aircraft oil breather application," *Proc. 2nd IEEE Int. Conf. Signals, Systems, Decision and Information Technology*, pp. 26-29, March 2003.
- [7] Z. Q. Zhu, Y. Pang, D. Howe, S. Iwasaki, R. Deodhar, and A. Pride, "Analysis of Electromagnetic Performance of Flux-Switching Permanent Magnet Machines by Nonlinear Adaptive Lumped Parameter Magnetic Circuit Model," *IEEE Transactions on Magnetics*, vol. 41, no. 11, pp. 4277-4287, July 2005.
- [8] K. Yamazaki, "Torque and efficiency calculation of an interior permanent magnet motor considering harmonic iron losses of both the stator and rotor," *IEEE Transactions on Magnetics*, vol. 39, no. 3, pp. 1460-1463, July 2003.
- [9] Tae Heoung Kim and Ju Lee, "Comparison of the Iron Loss of a Flux-Reversal Machine Under Four Different PWM Modes," *IEEE Transactions on Magnetics*, vol. 43, no. 4, pp. 1725-1728, April 2007.



Heung-Kyo Shin He received the B.S., M.S., and Ph.D. degrees in electrical engineering from Hanyang University, Seoul, Korea, in 1980, 1982 and 1990, respectively. Since 1988, he has been a Professor of Gyeongsang National University. In 2014, He was the chairman of Electrical Machinery & Energy Conversion Systems Society (EMECS) of KIEE, and from 2014 to 2015, vice-president of KIEE. His current research interests are the numerical analysis of electromagnetic fields and the design of electric machinery.